Evolution of Human Receptor Binding Affinity of H1N1 Hemagglutinins from 1918 to 2009 Pandemic Influenza A Virus

Nadtanet Nunthaboot,[†] Thanyada Rungrotmongkol,[‡,§] Maturos Malaisree,[‡] Nopporn Kaiyawet,[‡] Panita Decha,[||] Pornthep Sompornpisut,[‡] Yong Poovorawan,[⊥] and Supot Hannongbua*[,‡]

Department of Chemistry, Faculty of Science, Mahasarakham University, Mahasarakham, 44150, Thailand, Computational Chemistry Unit Cell, Department of Chemistry, Faculty of Science, Chulalongkorn University, Bangkok, 10330, Thailand, Center of Innovative Nanotechnology, Chulalongkorn University, Bangkok, 10330, Thailand, Computational Chemistry Research Unit, Department of Chemistry, Faculty of Science, Thaksin University, Phatthalung 93110, Thailand, and Center of Excellence in Clinical Virology, Faculty of Medicine, Chulalongkorn University, Bangkok, 10330, Thailand

Received January 27, 2010

The recent outbreak of the novel 2009 H1N1 influenza in humans has focused global attention on this virus, which could potentially have introduced a more dangerous pandemic of influenza flu. In the initial step of the viral attachment, hemagglutinin (HA), a viral glycoprotein surface, is responsible for the binding to the human SIA α2,6-linked sialopentasaccharide host cell receptor (hHAR). Dynamical and structural properties, based on molecular dynamics simulations of the four different HAs of Spanish 1918 (H1-1918), swine 1930 (H1-1930), seasonal 2005 (H1-2005), and a novel 2009 (H1-2009) H1N1 bound to the hHAR were compared. In all four HA−hHAR complexes, major interactions with the receptor binding were gained from HA residue Y95 and the conserved HA residues of the 130-loop, 190-helix, and 220-loop. However, introduction of the charged HA residues K145 and E227 in the 2009 HA binding pocket was found to increase the HA−hHAR binding efficiency in comparison to the three previously recognized H1N1 strains. Changing of the noncharged HA G225 residue to a negatively charged D225 provides a larger number of hydrogen-bonding interactions. The increase in hydrophilicity of the receptor binding region is apparently an evolution of the current pandemic flu from the 1918 Spanish, 1930 swine, and 2005 seasonal strains. Detailed analysis could help the understanding of how different HAs effectively attach and bind with the hHAR.

INTRODUCTION

The emerging influenza pandemic of the 2009 influenza A/H1N1 virus, with readily detected human−human transmission rates, has raised serious global concern for human health in recent times. Among the known targets determining the virus life's cycle, the initial step of viral attachment is mediated by HA binding the virion to the host cell receptor, α2,6 linked sialopentasaccharide (SIA-2,6-GAL; hHAR) in the case of humans. Amino acid mutations in the HA receptor binding domain could potentially introduce an outbreak of a new influenza virus. Relative to the 1918 Spanish (H1-1918), the 1930 swine (H1-1930), and the 2005 seasonal (H1-2005) H1N1 viruses, the HA binding pocket of the 2009 H1N1 (H1-2009) virus was found to display a notably higher hydrophilicity than the other three viral HAs. Such types of electronic effects, in cooperation with the structural differences due to the amino acid components (Table 1) in the binding pocket of the four HAs, are supposed to affect their susceptibility. A detailed and comparative understanding of the HA-hHAR binding among the four H1N1 strains is, then, the rational goal of this study.

On June 11, 2009, the WHO raised the alert status of the 2009 influenza A/H1N1 to level 6.[1] This novel H1N1 pandemic has caused at least 18 000 deaths in many countries around the world (as of July 2010). The most devastating influenza pandemic, 1918 H1N1 Spanish Flu, killed more than 40 million people worldwide.[2−4] The replication cycle of influenza virus is initiated by the attachment of the viral HA to sialylated glycans on the target cell-surface receptor, allowing for viral penetration into the host cell. While the adopted sialic acid α2,3-galactose linkage with a short glycan chain and cone-like topology is more favorable in avian influenza virus, the human and swine influenza viruses preferentially recognizes the sialic acid α2,6-galactose with longer glycan chains and an umbrella like topology,[5−10] hereafter referred to the hHAR. Besides HA functions, the M2-proton channel and neuraminidase (NA) are associated with the proton transport and the release of the newly synthesized viral particles in the viral replication cycle. Although the antiviral drugs approved against M2 ion channel and NA proteins are currently used for the treatment of influenza virus infections, the limitation of drug resistances because of amino acid mutations has led to an effort to

* To whom correspondence should be addressed. Tel: +66 22 187602. Fax: +66 22 187603. E-mail: supot.h@chula.ac.th.
[†] Department of Chemistry, Faculty of Science, Mahasarakham University.
[‡] Computational Chemistry Unit Cell, Department of Chemistry, Faculty of Science, Chulalongkorn University.
[§] Center of Innovative Nanotechnology, Chulalongkorn University.
[||] Computational Chemistry Research Unit, Department of Chemistry, Faculty of Science, Thaksin University.
[⊥] Center of Excellence in Clinical Virology, Faculty of Medicine, Chulalongkorn University.

10.1021/ci100038g
Published on Web 07/26/2010

Table 1. Comparison of Amino Acids in the HA Receptor Binding Domain of the Four Different H1N1 Influenza Viruses: The 1918 Spanish Flu (H1-1918), 1930 Swine Flu (H1-1930), 2005 Seasonal Flu (H1-2005), and 2009 Novel Flu (H1-2009)[a]

	H1N1 HA strains			
residue ID	H1-1918	H1-1930	H1-2005	H1-2009
95	Y	Y	Y	Y
133	T	T	**N**	**N**
133a	K	**R**	**R**	K
134	G	G	G	G
135	V	V	V	V
136	T	T	T	T
137	A	A	A	A
138	A	A	A	A
145	S	S	**N**	**K**
153	W	W	W	W
155	T	**V**	**V**	**V**
183	H	H	H	H
185	P	P	P	P
186	P	P	P	**S**
189	T	T	T	**A**
190	D	D	D	D
192	Q	Q	Q	Q
193	S	S	S	S
194	L	L	L	L
219	A	A	**E**	**I**
222	K	K	K	K
225	D	**G**	**G**	D
226	Q	Q	Q	Q
227	A	A	A	**E**
228	G	G	G	G

[a] Residues are numbered (residue ID) according to 1918 Spanish flu sequence. Using H1-1918 as the reference, the residue differences in the other three isolates are shown in bold and underlined. Residue K133a is an inserted amino acid specific to H1.

discover new potent inhibitors. Impacts of drug-resistant mutant strains of these two targeted proteins and their relevant commercial agents have been extensively studied.[11−14]

The viral genetic sequences in the HA receptor binding domain of the four different H1N1 influenza viruses, that is, the 1918 Spanish flu, 1930 swine flu, 2005 seasonal flu, and 2009 novel flu, are compared and are summarized in Table 1 (see multiple sequence alignment in Figure S1, Supporting Information). Using the original 1918 H1N1 HA as the reference, the amino acids at 7 Å spherical radius around the hHAR in the binding pockets of the H1-1930, H1-2005, and H1-2009 HAs contain three (K133aR, T155V, and D225G), six (T133N, K133aR, S145N, T155V, A219E, and D225G), and seven (T133N, S145K, T155V, P186S, T189A, A219I, and A227E) substitutions (shown in bold and underlined in Table 1), respectively. From a comparison of the hydrophobic plots (Figure 1), the 2009 HA binding pocket displays considerably higher hydrophilic characteristics (represented by the blue surface) than those of the other three HA strains. Since the residues 190 and 225 are known to be a key factor determining the HA−hHAR binding in all H1N1 subtypes,[15−20] and the HAs of all H1N1 strains contain D190, therefore, interest is focused on residue 225 in which G225 was found in the 1930 swine and 2005 seasonal viruses, whereas D225 was detected in the HAs of the two pandemic strains, H1-1918 and H1-2009 (Table 1). In addition, residue A227, which is the receptor binding site that is commonly conserved as "Q226-A227-G228" (QAG) was replaced by E227 in the novel 2009 influenza virus. Substitution of A227 by the negatively charged E227 residue (QEG) is supposed to affect the orientation of the surrounding residues.[18] As a consequence, the increase of the hydrophilicity and the replacement of the QAG by the QEG receptor binding site of the H1-2009 HA are possibly involved in the recognition and familiarity-strength in the binding to the hHAR of the newly emerged flu.

To examine the influence of the electronic and structural changes in the four HA binding pockets, molecular dynamics (MD) simulations of the hHAR bound to the four HA A/H1N1 influenza viruses were carried out. The HA−hHAR binding, as well as the structural and dynamical properties, were analyzed and are extensively discussed. The observed information at the atomic level could essentially provide a better understanding and a prediction of the new H1N1 influenza pathogenesis.

MATERIALS AND METHODS

System Preparation. The cocrystal structure of the 1930 swine influenza A/H1N1 HA (H1-1930) with the hHAR and the crystal structure of the apo form of the 1918 influenza A/H1N1 HA (H1-1918), were retrieved from the Protein Data Bank (PDB entry codes 1RVT and 1RUZ, respectively)[21] and were used as the starting structures for the MD simulations. To prepare the hHAR bound to the H1-1918 HA, superposition of the H1-1930 and the H1-1918 HA proteins over the backbone carbon atoms was performed, and the H1-1930 coordinates were then removed, retaining the coordinates of hHAR. The structure of the 2005 seasonal H1N1 HA complexed with the hHAR was prepared in a similar fashion of the H1-2009.[22] Briefly, using the structure of 1930 swine flu[21] as a template and amino acid sequences of the isolated Influenza A/swine/Chachoengsao/NIAH587/2005(H1N1),[23] the 3D-structure of the 2005 HA protein was created by homology modeling technique using the module implemented in Discovery Studio 2.0.[24] The hHAR bound to the H1-2005 HA was set up in a similar manner to that of the aforementioned H1-1918.

Molecular Dynamics Simulations. All calculations of the HA-hHAR complexes were carried out using the AMBER 10 software package.[25] The HA proteins and the hHAR were parametrized using the AMBER03[26] and GLYCAM06 force fields,[27] respectively. Protonation of the ionizable amino acids was assigned at pH 7.0 using the PROPKA program.[28,29] All missing hydrogen atoms were added using the LEaP module implemented in AMBER 10.[25] The simulated system was subsequently solvated by TIP3P water molecules in a cubic box with dimensions of $65 \times 68 \times 143$ Å^3 for H1-1918, $65 \times 68 \times 141$ Å^3 for H1-1930, and $67 \times 68 \times 141$ Å^3 for H1-2005. This is almost comparable to that of $66 \times 69 \times 141$ Å^3 used before for the H1-2009 complex.[22] The electroneutrality of the simulated systems was treated by adding 1, 0, 4, and 5 chloride counterions for H1-1918, H1-1930, H1-2005, and H1-2009, respectively. The periodic boundary condition in the isobaric−isothermal (NPT) ensemble with a constant pressure of 1 atm and temperature of 310 K was set up, whereas a Berendsen coupling time of 0.2-ps was employed to control the temperature. Nonbonded interactions were calculated with a 12 Å residue-based cutoff, and the Particle Mesh Ewald method[30] was applied to treat the long-range electrostatic interactions. A 2-fs step size with the SHAKE algorithm[31] was used along the simulations.

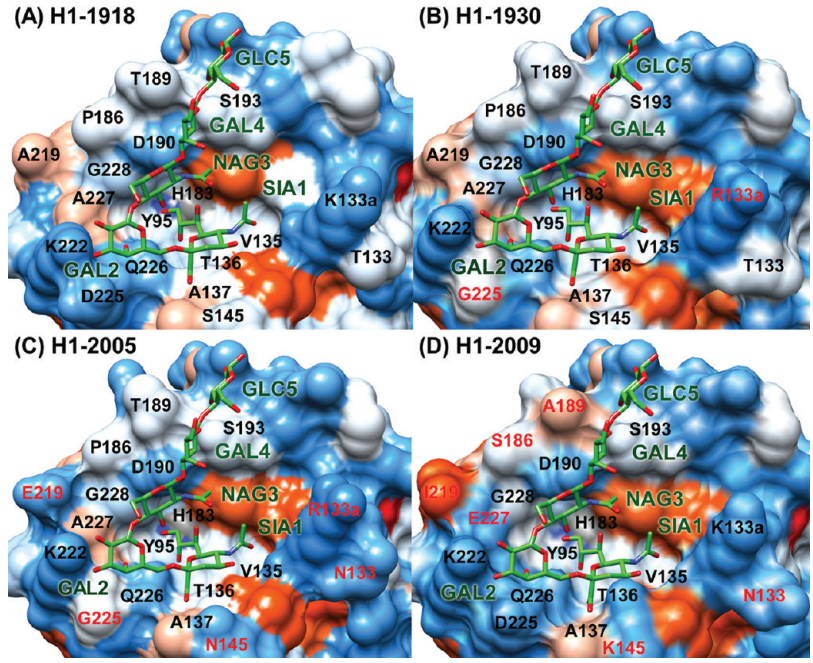

Figure 1. The hHAR in the binding pocket of the four viral influenza A/H1N1 HAs: (A) 1918 Spanish flu (H1-1918), (B) 1930 swine flu (H1-1930), (B) 2005 seasonal flu (H1-2005), and (D) 2009 novel pandemic flu (H1-2009). For H1-1930, H1-2005, and H1-2009, the residues that differ from the reference H1-1918 sequence are shown in red. The hydrophilic and hydrophobic surfaces are colored by blue and orange, respectively.

The water molecules were first relaxed with 500 steps of steepest descent (SD) and 1000 steps of conjugated gradient minimizations, while the HA and hHAR coordinates were kept fixed. The whole system was consequently optimized by performing 1,000 steps of SD and 1,000 steps of conjugated gradient minimizations. Afterward, the systems was heated to 310 K over 100-ps simulation and pre-equilibrated for 400 ps with position restraints on the hHAR atoms with factors of 20 and 10 kcal·mol^{-1}·Å^{-2} to maintain their coordinates inside the receptor-binding pocket. Finally, 6.5-ns simulations were carried out for each HA-hHAR complex and the structural coordinates from the last 5-ns (1.5−6.5-ns) simulations, a production period, were collected for analysis.

RESULTS AND DISCUSSION

Changes of the Receptor Conformation Inside the H1 Binding Pocket. The attachment of the viral surface homotrimeric glycoprotein HA to the host membrane via the hHAR is believed to be the primary step in the viral replication cycle. To differentiate the receptor's conformation in the binding pocket of the HAs of the Spanish flu (H1-1918), swine flu (H1-1930), seasonal flu (H1-2005), and a novel pandemic flu (H1-2009), the distributions of the torsion angles ($\tau1-\tau9$ in Figure 2) were measured and are plotted in Figure 3. As defined in Figure 2, $\tau1-\tau9$ were classified in three important regions providing three different characters of the receptor binding: (i) $\tau1-\tau3$, conformations of terminal sialic acid (SIA1) α2,6-linked to galactose (GAL2) of the hHAR; (ii) $\tau4-\tau6$, orientations of the three side chains of the SIA1 functional groups; and (iii) $\tau7-\tau9$, bridging between the saccharide units 2−5 of the receptor.

The distributions of the torsion angle plots (Figure 3), excluding $\tau9$ of H1-1930 and $\tau4$ of H1-2005, reveal clearly that all torsion angles of the four HA-hHAR systems show a sharp peak at almost the same position, suggesting that the hHAR adapts itself very well to reach its optimal structure within the four H1NI HA binding sites.

The $\tau1-\tau3$ angles on the single bonds linking between the six-membered rings of the SIA1 terminus and the GAL2 unit show a sharp peak at approximately −65°, −165° and 70°, respectively, indicating an identical orientation of these two sugars puckered into the HA pocket site. The $\tau1$ glycosidic torsion of approximately −65° represents their cis-conformation on the α-ketosidic linkage corresponding to those commonly observed in the SIA-α2,6-GAL receptor (hHAR) bound to other HAs by both experimental and theoretical studies.[21,32−35] Considering the orientations of the three side chains of the SIA1, the difference was only found at the carboxylate group of the H1-2005 in which its $\tau4$ was detected at ∼30° relative to ∼180° for the other HAs, that is, in difference from the other systems, the O1A group (see Figure 2) of the H1-2005 was rotated into the binding site to interact with the HA residues. The $\tau6$ angle of the hydrophilic moiety displayed a sharper peak than the $\tau4$ of the $-COO^-$ and $\tau5$ of the −NHAc groups, indicating that these two side chains are slightly more flexible in a narrow range in comparison with the hydrophilic group of the terminal SIA1.

For the remaining sugar moieties lying on the surface-exposed region of the hHAR protein (see Figure 1), the structural conformations of the NAG3 and GAL4 were found to be similar among the four HAs, as presented by the same degrees of $\tau7$ and $\tau8$ angles (−70° and −80°, respectively, in Figure 3). However, the orientation of the last glycan unit, GLC5, in the H1-1930 ($\tau9$ of 65°, red line) was somewhat different from the other three HAs ($\tau9$ of −65°). Therefore, different intermolecular interactions of the terminal GLC5 sugar of the saccharide chain with the protein surface residues

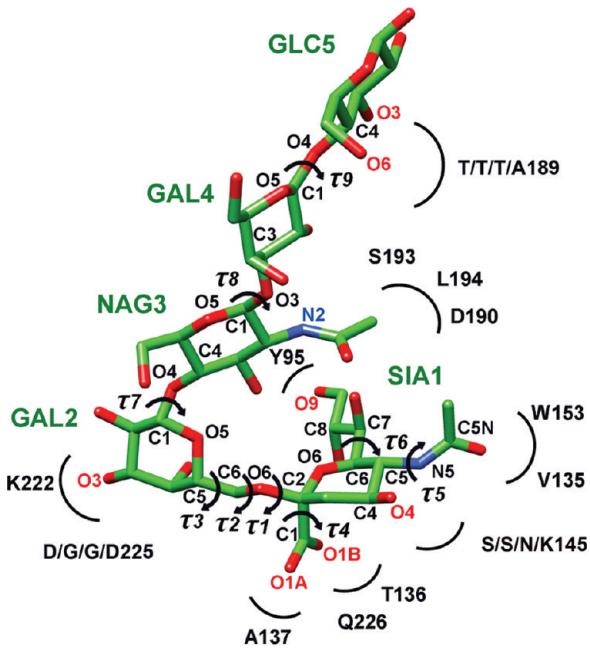

Figure 2. Schematic representation and definitions of the $\tau 1-\tau 9$ torsion angles of the hHAR in the binding site of the HA subtype H1. Some labeled atoms used in the results and discussion are also shown. The labels, such as S/S/N/K145, were used to represent the four different amino acids in the same sequence number of the 1918-, 1930-, 2005- and 2009-H1N1 HAs, respectively.

are to be expected in the H1-1930 case (details in the following sections).

Enzyme−Receptor Interactions. To gain insight into the efficiency of the hHAR binding to the HAs of H1-1918, H1-1930, H1-2005, and H1-2009, the percentage and number of hydrogen bonds between this receptor and the contact residues of HAs were measured according to the subsequent criteria: (i) the distance between proton donor (D) and acceptor (A) atoms of ≤3.5 Å and (ii) the D−H···A angle of ≥120°. The results are shown in Figure 4 and the hydrogen bond descriptions are given in Table S1 (Supporting Information).

As shown in Figure 4, hydrogen bonds between the hHAR and the HA residues in all systems can be firmly formed in the three important binding HA regions, 130-loop, 190-helix, and 220-loop, especially at the sialic acid terminus which is inserted directly into the receptor-binding pocket of the HA. Strong hydrogen bonds are almost conserved at the residues Y95, V135, T136, A137, and Q226 of the four HA strains. Note that major interactions between the SIA1 and the T136 and Q226 are maintained although different hydrogen bonding pattern was detected, that is, the interaction takes

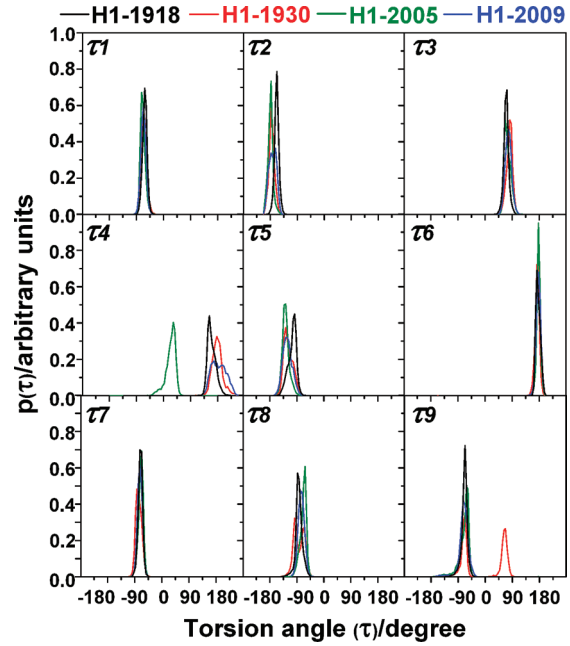

Figure 3. Distribution plots of the torsion angles ($\tau 1-\tau 9$) of the hHAR lying within the binding pocket of the HA of the four H1N1 strains (H1-1918, H1-1930, H1-2005, and H1-2009).

place via the O1A in the H1-2005 and the O1B in the other HAs (see Table S1, Supporting Information). Noticeably change was found when the S/S/N145, a polar residue with noncharged side chain, in the H1-1918, H1-1930, and H1-2005 was replaced by the K145, a positively charged residue in a novel HA. This makes the H1-2009 capable of establishing one moderate hydrogen bond to the O4 of SIA1. The observed results lead to conclusion that introducing of the fourth lysine (K145) of the lysine fence (K133, K156, and K222) in the HA of the 2009 facilitates stronger enzyme−receptor binding by better anchoring the SIA1 terminus. This observation is in agreement with the recently proposed hypothesis.[36] Furthermore, a strong hydrogen bond between the H183 and the O9 of SIA1 was observed in the H1-1930, H1-2005, and H1-2009 complexes, whereas this kind of interaction was disappeared in the case of H1-1918 system.

A major difference was additionally found at the connecting GAL2 unit, where the number and percentage of hydrogen bonding interactions detected at the HA 220-loop on residues K222 and D/G/G/D225 are much stronger for H1-1918 and H1-2009 than those of H1-1930 and H1-2005 (Figure 4). It is clear that for the D/G/G/D225 binding, the direct electrostatic effects because of the negatively charged D225 residue, lead to a more effective interaction in the H1-1918 and the H1-2009 viral HAs than the noncharged G225 in the HA of the H1-1930 and H1-2005 viruses. For the K222-GAL2 binding, the moderate and strong hydrogen bonds between O3 of this particular unit and the K222 residue in the HA of H1-1918 and H1-2009 were observed. This is possibly affected by the indirect effects caused by the presence of one (D225) and two (D225 and E227) negatively charged residues (see also Table 1) in the binding pocket of H1-1918 and H1-2009, respectively. In 2009 influenza pandemic strain, the orientation of the K222 residue was mainly stabilized by both D225 and E227 residues through electrostatic and salt-bridge interactions, respectively

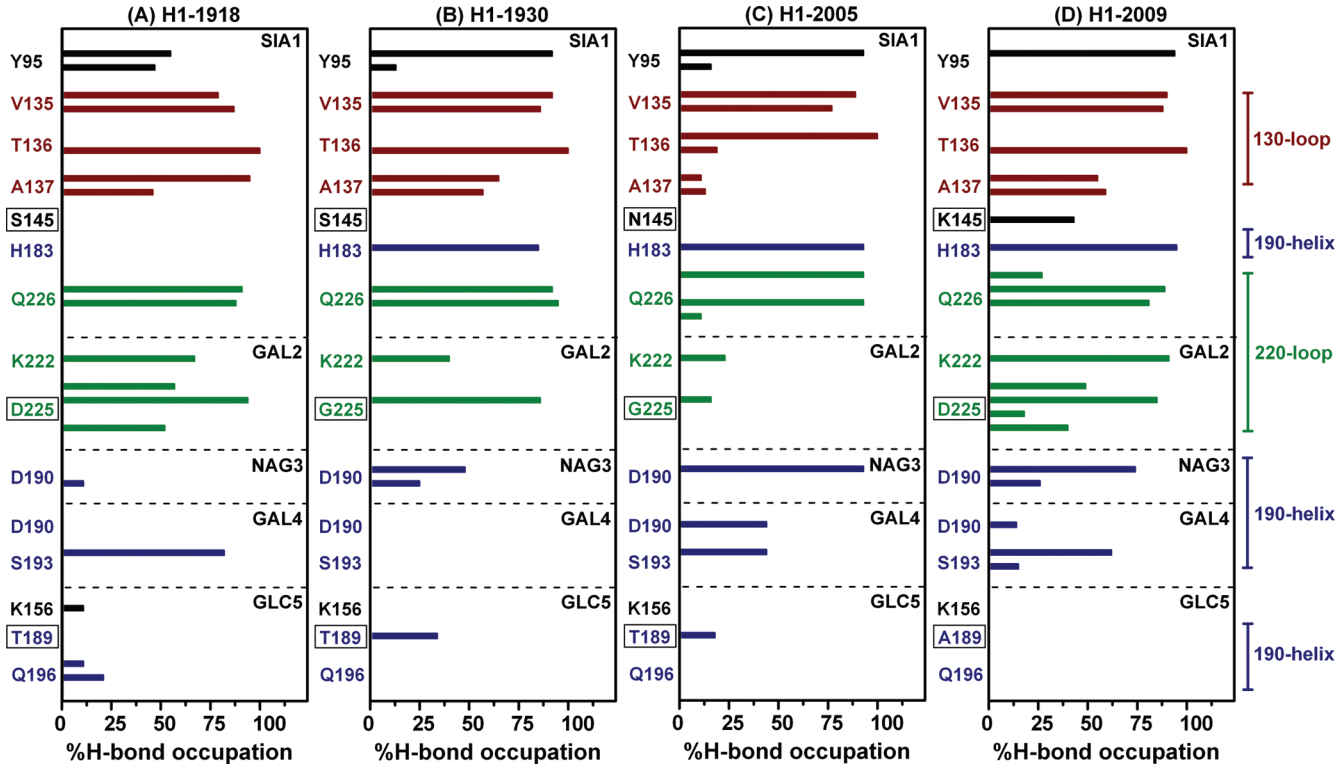

Figure 4. Hydrogen bond occupation between the five saccharide units (SIA1, GAL2, NAG3, GAL4, and GLC5) of the hHAR and the HA binding residues of (A) Spanish flu (H1-1918), (B) swine flu (H1-1930), (C) seasonal flu (H1-2005), and (D) a novel flu (H1-2009). The residues which are different among the four HAs are shown with a box around the label (see Figure 1 for residue positions). Residues of the 130-loop, 190-helix, and 220-loops are colored by red, blue, and green, respectively.

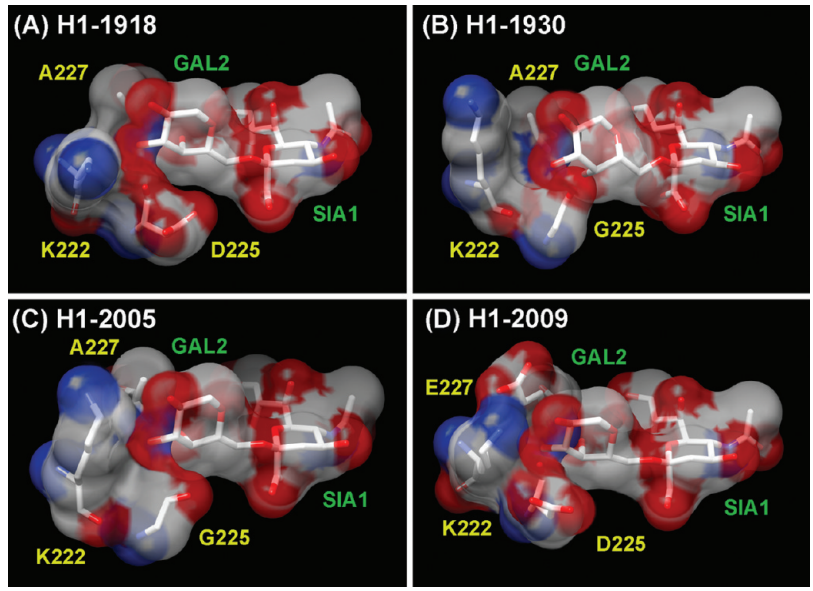

Figure 5. Electrostatic potential map of hHAR and HA binding residues K222, D/G/G/D225 and A/A/A/E227 of (A) Spanish flu (H1-1918), (B) swine flu (H1-1930), (C) seasonal flu (H1-2005), and (D) novel flu (H1-2009). Positive and negative electrostatic potentials are represented by blue and red, respectively.

(see Figure 5D and more discussion in the next section), whereas only D225 was observed to stabilize K222 in the case of H1-1918. This is in contrast with what was found for the H1-1930 and H1-2005 viruses, where both the G225 and A227 residues are hydrophobic, leading to a lowering of the electrostatic potential in this region, relative to those of the other two systems. This provides a clear reason why K222 could not form a stable hydrogen bond with GAL2 in the H1-1930 and H1-2005 HAs (Figure 4B and C, respectively). This hypothesis is further analyzed in terms of the electrostatic potential plot in the next section. A crucial role of residue 225 has been reported previously,[16−18] with the additional hypothesis that mutation of this residue could result in a reduced viral binding affinity to the hHAR. It has also been experimentally found that the presence of the G225 residue in the HA of H1-1930 and H1-2005 apparently reduced the binding efficiency of the virus to the hHAR.[3,16,18]

With respect to the NAG3, GAL4, and GLC5 saccharide units, which lay on the surface exposed region (Figure 1), far from the binding pocket, and are supposed to play only

a minor role in holding the receptor in place, a lower percentage and number of hydrogen bonds were found (Figure 4) in comparison to those observed at the first two units (SIA1 and GAL2) of the receptor. Their interactions were moderately strong with 190-helix residues T/T/T/A189, D190, and S193.

Taking into account all the above given data, the order of hydrogen bond strengths of the hHAR binding to the H1N1 HAs was H1-2009 > H1-1918 > H1-2005 ≅ H1-1930. The increase of binding affinity in the novel H1-2009 (H1N1) HA to the hHAR is mainly because of the higher hydrophilicity at the receptor binding domain, in which residues 145, 225, and 227 were found to play a critical role. The transmissibility of the 2009 H1N1 virus (depending upon several external factors and determined by the basic reproduction number, R_0 of 1.2−1.6) falls within the range of the 1918 Spanish flu (R_0 of 1.4−2.8) but is higher than that of seasonal influenza virus (R_0 of 0.9−2.1).[37,38] This transmission ability is supposed to relate, somewhat, to the predicted enzyme-receptor binding affinity. Note that the pathogenesis and transmission studies of the 2009 H1N1 influenza virus indicated that a novel flu was observed to be more pathogenic than the seasonal H1N1 virus.[38,39] Since the 2009 influenza virus could deeply penetrate into the airways and exhibits more extensive viral replication in the respiratory tract, its severity could potentially increase in comparison with seasonal virus.[38,39]

Effect of Charged Residues on the Receptor Binding Affinity. As already mentioned, hydrogen bond analysis revealed that introduction of charged amino acids in the receptor binding domain of the novel HA influenza virus could effectively contribute to the binding with the hHAR, in particular HA residues 222, 225, and 227. Therefore, to provide an additional perspective on the contribution of the polar residues to the hHAR-HA binding, the electrostatic isosurface maps of the hHAR and the HA 222, 225, and 227 residues were plotted in Figure 5. The positive and negative electrostatic potentials are indicated by blue and red, respectively.

In all systems, the negative electrostatic potentials (Figure 5, red) were found around the SIA1 and GAL2 units of the hHAR, while a positive electrostatic potential was generated over the K222 residue (Figure 5, blue). Differences between the four viral HAs are clearly and obviously observed in the region around the 225 and 227 residues. Here, changing the negatively charged D225 residue in the 1918- and 2009-H1N1 models to a nonpolar G225 residue (Table 1) leads to the negative electrostatic potential around residue 225 almost totally disappearing (the red regions in Figure 5A and D change to white in Figure 5B and C, respectively). In addition, the substitution of a nonpolar A227 residue of the 1918-, 1930-, and 2005-H1N1 HAs (Table 1) with a negatively charged E227 residue in the HA of H1-2009 leads additionally to an enhanced negative electrostatic potential around the 227 residue (the red region, which is only observed in Figure 5D).

As a consequence, the electrostatically negative potentials near residues D225 and E227 are unique in the H1-2009 H1N1 isolate (of the four studied) and the enhanced electronegative isosurface could potentially stabilize the ionic network of the 220-loop residues K222, D225, and E227. This helps the K222 residue to adjust its conformation to be in optimal contact with the GAL2 moiety of the hHAR, leading to the formation of a strong hydrogen bond in the H1-2009 HA−hHAR complex (Figure 4D), as previously discussed. On the other hand, the electrostatic potentials that result from the combination of the charged- and noncharged residues (D225 and A227) can potentially induce the moderate K222−GAL2 hydrogen bond formation in the H1-1918 HA−hHAR interaction (Figure 4A). This is not the case for the H1-1930 and H1-2005 HAs (Figure 4B and C, respectively), where this hydrogen bond is very weak because both G225 and A227 are fully uncharged and could not establish such ionic network with the K222.

Role of the Nonconserved Residue 227. Although residue 227 was found to vary between the influenza A viral strains, the receptor binding residues Q226 and G228 are highly conserved, forming a "Q226-X227-G228" pattern or so-called "QXG" site, where QSG and QGG sites are found in the avian H3 or H5 and H2 influenza virus HAs, respectively.[18,40] In this study, both the 1918-, 1930-, and 2005-H1N1 strains contain the QAG sequences, whereas the 2009-novel flu (H1-2009) shows a unique QEG site. The increased hydrophilicity in the receptor binding region is apparently the development of the current pandemic flu from the 1918 Spanish, the 1930 swine, and the seasonal 2005 influenzas. As shown and described in the previous sections, substitution of the noncharged A227 residue with the negatively charged E227 improves the binding of HA to the hHAR, and this is potentially attained by establishing the ionic network with the K222 and D225 residues. This finding thus indicates that the nonconserved residue 227 possibly plays a critical role in the evolution of a new and potentially more pathogenic H1N1 influenza virus. Note that among the three residues in the HA QXG site of the four H1 strains under this study, Q226 is the only residue that interacts directly with the hHAR via strong hydrogen bonds (Figure 4).

Human HAR Solvation. Solvation of the hHAR was monitored in terms of atom−atom radial distribution functions, RDFs, $g_{xy}(r)$, the probability of finding a particle of type y within a sphere radius r around the particle of type x. The RDFs from all heteroatoms of the hHAR to the oxygen atom of water were evaluated. The selected RDFs and the corresponding running coordination numbers, $n(r)$, are shown in Figure 6.

For all HA-hHAR complexes, the major differences in the $g(r)$ at the SIA1 terminus takes place only on the O1B atom (see Figure 2 for atomic label), where the plot for the H1-2005 complex shows the first sharp peak at ∼2.7 Å with the corresponding coordination number $n(r)$ integrated up to its first minimum of 2.8 water molecules (Figure 6B, right axis). This indicates that the water was firmly coordinated to the O1B atom of the H1-2005, but not in the HA-hHAR systems of H1-1918, H1-1930, and H1-2009. This is because of the interchange of the O1A and O1B positions due to the rotation of the $\tau 4$ angle (see Figure 3).

Although no significant difference was found in terms of the peak position of the RDFs of the other atoms of the SIA1 (Figure 6A, C, and D), the $n(r)$ of the H1-1918, H1-1930, and H1-2005 show a higher average number of water molecules located around this glycan unit than that detected in the H1-2009. In other words, the SIA1 of the hHAR in the HA−hHAR complex of the H1-2009 virus is less solvated than that with the other three HAs. This is consistent with the hydrogen bond

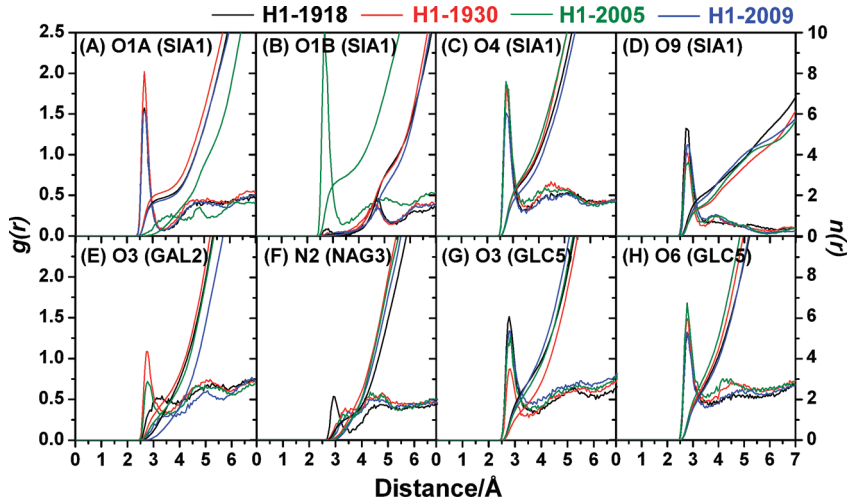

Figure 6. Radial distribution function, $g(r)$, centered on the selected heteroatoms of the hHAR (see Figure 2 for atomic labels) to oxygen atoms of water molecules and the running coordination number, $n(r)$, for the four simulated HA−hHAR systems.

data (Figure 4), where a greater level of direct contact leads to the formation of more hHAR−HA hydrogen bonds with the H1-2009 than with the other three viral strains. A clear example is the moderate hydrogen bonding between the O4 atom of SIA1 of the hHAR and the guanidinium group of the HA K145 residue that only takes place in H1-2009 (Figure 4D). Another example that supports the degree of the solvation of O9 atom (Figure 6D) is the strong hydrogen bonding between this oxygen and the HA H183 residue, which is in a reverse order of the first shell coordination numbers for O9 of 1.5 1.5, 2.0, and 2.5 water molecules for H1-2005, H1-1930, H1-2009, and H1-1918, respectively.

For the other four glycan units, the following significant differences were found: O3 of GAL2 (Figure 6E), N2 of NAG3 (Figure 6F), and O3 of GLC5 (Figure 6G), in which the degree of solvation also supports the hydrogen bond data discussed previously (Figure 4).

CONCLUSION

In the present work, MD simulations of the hHAR bound to the four different HAs of the 1918-, 1930-, 2005-, and 2009-H1N1 influenza viruses were studied and compared in terms of hydrogen bond formation, receptor conformational changes, the role of the receptor binding residues and the receptor solvation level.

In all complexes, the glycosidic torsion angle linking the terminal sialic acid and the adjoining GAL2 of apprximately −65° confirmed the preferentially favorable cis-conformation of the hHAR, similar to that detected with other HA strains.[34,35] The SIA1 terminus was found to interact strongly with the HA Y95 residue and with the conserved residues of the HA receptor binding domain, which consists of the 130-loop (V135, T136 and A137), 190-helix (H183, except for H1-1918), and 220-loop (K222 and Q226) through many strong hydrogen bonds, whereas the GAL2 and the last three glycan units (NAG3, GAL4 and GLC5) of the hHAR established hydrogen bonds with amino acids in the HA 220-loop and 190-helix, respectively. More importantly, the crucial presence of a positively charged K145 residue in the HA of the novel H1-2009 can potentially make a lysine fence with residues K133, K156, and K222 and provides an optimal contact to hydrogen bond with the SIA1 of the hHAR. Because of the presence of an uncharged S/S/N145 residue in place of the K145, such an ionic network was not created in the Spanish 1918, swine 1930, or seasonal 2005 virions, resulting in the lower potency of HA−hHAR binding. As observed in the all H1N1 strains,[15,18,20] HA residue 225 plays a critical role in the hHAR GAL2 binding efficiency. The presence of a negatively charged D225 residue in the HAs of the H1-1918 and H1-2009 could provide a larger number of hydrogen bonds in the HA−hHAR complex than that observed in H1-1930 and H1-2005, where a noncharged G225 residue exists instead. Q226 of the QAG (1918-, 1930-, and 2005-H1N1) or QEG (2009-H1N1) HA sequence directly interacts with the hHAR SIA1 terminus via hydrogen bonds, while the nonconserved 227 residue was found to play a role in stabilizing the enzyme structure around the K222 residue. Introduction of the negatively charged HA E227 residue in the H1-2009 substantially enhanced the HA−hHAR binding efficiency through hydrogen bonds formation between the HA K222 residue and the GAL2 unit of the hHAR. The lower hydrogen bonding interactions in the H1-1918, H1-1930, and H1-2005 HAs were compensated by a higher degree of water accessibility to the hHAR.

In conclusion, the efficiency of the hHAR binding to the HA of the novel 2009 H1N1 viral strain is greater than that in the 1918 Spanish and the 2005 seasonal (which is comparable to the 1930 swine) influenza viruses, respectively. A major contribution to the virion HA-cellular hHAR binding in H1-2009 is apparently gained from the charged residues existing in the HA binding pocket. Our simulated results provide a better understanding of how the viral surface glycoprotein HA of different H1N1 strains efficiently attach and bind to the hHAR.

ACKNOWLEDGMENT

This work was financially supported by the Thailand Research Fund (TRF), the Commission Higher Education (CHE), and the Thai Government Stimulus Package 2 (TKK2555), under the Project for Establishment of Comprehensive Center for Innovative Food, Health Products and Agriculture. N.N. (grant No. MRG5180298) and T.R. (grant No. TRG5280035) acknowledge the TRF grant for the new research. P.S. gratefully acknowledges the support from the Emerging Diseases and Bio-Warefare project, the Center of Excellence in Clinical Virology, Chulalongkorn University.

Supporting Information Available: Multiple sequence alignment of all four H1N1 strains and hydrogen bond descriptions. This information is available free of charge via the Internet at http://pubs.acs.org/.

REFERENCES AND NOTES

(1) World Health Organization. Global Alert and Response (GAR). http://www.who.int/csr/disease/swineflu/en/index.html (accessed July 10, 2010).

(2) Neumann, G.; Noda, T.; Kawaoka, Y. Emergence and pandemic potential of swine-origin H1N1 influenza virus. *Nature* **2009**, *459*, 931–939.

(3) Shen, J.; Ma, J.; Wang, Q. Evolutionary trends of A(H1N1) influenza virus hemagglutinin since 1918. *PLoS One* **2009**, *4*, e7789.

(4) Krug, R. M.; Aramini, J. M. Emerging antiviral targets for influenza A virus. *Trends Pharmacol. Sci.* **2009**, *30*, 269–277.

(5) Chandrasekaran, A.; Srinivasan, A.; Raman, R.; Viswanathan, K.; Raguram, S.; Tumpey, T. M.; Sasisekharan, V.; Sasisekharan, R. Glycan topology determines human adaptation of avian H5N1 virus hemagglutinin. *Nat. Biotechnol.* **2008**, *26*, 107–113.

(6) Bateman, A. C.; Busch, M. G.; Karasin, A. I.; Bovin, N.; Olsen, C. W. Amino acid 226 in the hemagglutinin of H4N6 influenza virus determines binding affinity for 2,6-linked sialic acid and infectivity levels in primary swine and human respiratory epithelial cells. *J. Virol.* **2008**, *82*, 8204–8209.

(7) Gambaryan, A. S.; Karasin, A. I.; Tuzikov, A. B.; Chinarev, A. A.; Pazyninab, G. V.; Bovinb, N. V.; Matrosovich, M. N.; Olsen, C. W.; Klimove, A. I. Receptor-binding properties of swine influenza viruses isolated and propagated in MDCK cells. *Virus. Res.* **2005**, *114*, 15–22.

(8) Matrosovich, M. N.; Gambaryan, A. S.; Teneberg, S.; Piskarev, V. E.; Yamnikova, S. S.; Lvov, D. K.; Robertson, J. S.; Karlsson, K. A. Avian influenza A viruses differ from human viruses by recognition of sialyloligosaccharides and gangliosides and by a higher conservation of the HA receptor-binding site. *Virology* **1997**, *23*, 224–234.

(9) Rogers, G. N.; D'Souza, B. L. Receptor binding properties of human and animal H1 influenza virus isolates. *Virology* **1989**, *173*, 317–322.

(10) Bewley, C. A. Illuminating the switch in influenza viruses. *Nat. Biotechnol.* **2008**, *26*, 60–62.

(11) Laohpongspaisan, C.; Rungrotmongkol, T.; Intharathep, P.; Malaisree, M.; Decha, P.; Aruksakunwong, O.; Sompornpisut, P.; Hannongbua, S. Why amantadine loses its function in influenza M2 mutants: MD simulations. *J. Chem. Inf. Model.* **2009**, *49*, 847–852.

(12) Ghosh, A.; Nandy, A.; Nandy, P.; Gute, B. D.; Basak, S. C. Computational study of dispersion and extent of mutated and duplicated sequences of the H5N1 influenza neuraminidase over the period 1997−2008. *J. Chem. Inf. Model.* **2009**, *49*, 2627–2638.

(13) Udommaneethanakit, T.; Rungrotmongkol, T.; Bren, U.; Frecer, V.; Stanislav, M. Dynamic behavior of avian influenza A virus neuraminidase subtype H5N1 in complex with oseltamivir, zanamivir, peramivir, and their phosphonate analogues. *J. Chem. Inf. Model.* **2009**, *49*, 2323–2332.

(14) Rungrotmongkol, T.; Intharathep, P.; Malaisree, M.; Nunthaboot, N.; Kaiyawet, N.; Sompornpisut, P.; Payungporn, S.; Poovorawan, Y.; Hannongbua, S. Susceptibility of antiviral drugs against 2009 influenza A (H1N1) virus. *Biochem. Biophys. Res. Commun.* **2009**, *385*, 390–394.

(15) Glaser, L.; Stevens, J.; Zamarin, D.; Wilson, I. A.; García-Sastre, A.; Tumpey, T. M.; Basler, C. F.; Taubenberger, J. K.; Palese, P. A single amino acid substitution in 1918 influenza virus hemagglutinin changes receptor binding specificity. *J. Virol.* **2005**, *79*, 11533–11536.

(16) Stevens, J.; Blixt, O.; Tumpey, T. M.; Taubenberger, J. K.; Paulson, J. C.; Wilson, I. A. Structure and receptor specificity of the hemagglutinin from an H5N1 influenza virus. *Science* **2006**, *312*, 404–410.

(17) Taubenberger, J. K. Influenza hemagglutinin attachment to target cells: "Birds do it, we do it". *Future Virol.* **2006**, *1*, 415–418.

(18) Matrosovich, M.; Tuzikov, A.; Bovin, N.; Gambaryan, A.; Klimov, A.; Castrucci, M. R.; Donatelli, I.; Kawaoka, Y. Early alterations of the receptor-binding properties of H1, H2, and H3 avian influenza virus hemagglutinins after their introduction into mammals. *J. Virol.* **2000**, *74*, 8502–8512.

(19) Yang, Z. Y.; Wei, C. J.; Kong, W. P.; Wu, L.; Xu, L.; Smith, D. F.; Nabel, G. J. Immunization by avian H5 influenza hemagglutinin mutants with altered receptor binding specificity. *Science* **2007**, *317*, 825–828.

(20) Stevens, J.; Blixt, O.; Glaser, L.; Taubenberger, J. K.; Palese, P.; Paulson, J. C.; Wilson, I. A. Glycan microarray analysis of the hemagglutinins from modern and pandemic influenza viruses reveals different receptor specificities. *J. Mol. Biol.* **2006**, *355*, 1143–1155.

(21) Gamblin, S. J.; Haire, L. F.; Russell, R. J.; Stevens, D. J.; Xiao, B.; Ha, Y.; Vasisht, N.; Steinhauer, D. A.; Daniels, R. S.; Elliot, A.; Wiley, D. C.; Skehel, J. J. The structure and receptor-binding properties of the 1918 influenza hemagglutinin. *Science* **2004**, *303*, 1838–1842.

(22) Nunthaboot, N.; Rungrotmongkol, T.; Malaisree, M.; Decha, P.; Kaiyawet, N.; Intharathep, P.; Sompornpisut, P.; Poovorawan, Y.; Hannongbua, S. Molecular insights into human receptor binding to 2009 H1N1 influenza A hemagglutinin. *Monatsh. Chem.* **2010**, *141*, 801–807.

(23) Influenza virus resource. http://www.ncbi.nlm.nih.gov/genomes/FLU/SwineFlu.html (accessed Apr 25, 2009).

(24) *Discovery Studio 2.0*; Accelrys Inc: San Diego, CA, 2007.

(25) Case, D. A.; Darden, T. A.; Cheatham, III, T. E.; Simmerling, C. L.; Wang, J.; Duke, R. E.; Luo, R.; Crowley, M.; Walker, R. C.; Zhang, W.; Merz, K. M.; Wang, B.; Hayik, S.; Roitberg, A.; Seabra, G.; Kolossváry, I.; Wong, K. F.; Paesani, F.; Vanicek, J.; Wu, X.; Brozell, S. R.; Steinbrecher, T.; Gohlke, H.; Yang, L.; Tan, C.; Mongan, J.; Hornak, V.; Mathews, G. C. D. H.; Seetin, M. G.; Sagui, C.; Babin, V.; Kollman, P. A. *AMBER10*; University of California: San Francisco, CA, 2008.

(26) Duan, Y.; Wu, C.; Chowdhury, S.; Lee, M. C.; Xiong, G.; Zhang, W.; Yang, R.; Cieplak, P.; Luo, R.; Lee, T.; Caldwell, J.; Wang, J.; Kollman, P. A point-charge force field for molecular mechanics simulations of proteins based on condensed-phase quantum mechanical calculations. *J. Comput. Chem.* **2003**, *24*, 1999–2012.

(27) Tessier, M. B.; Demarco, M. L.; Yongye, A. B.; Woods, R. J. Extension of the GLYCAM06 biomolecular force field to lipids, lipid bilayers and glycolipids. *Mol. Simulat.* **2008**, *34*, 349–364.

(28) Li, H.; Robertson, A. D.; Jensen, J. H. Very fast empirical prediction and rationalization of protein pKa values. *Proteins* **2005**, *61*, 704–721.

(29) Bas, D. C.; Rogers, D. M.; Jensen, J. H. Very fast prediction and rationalization of pKa values for protein-ligand complexes. *Proteins* **2008**, *73*, 765–783.

(30) Darden, T.; York, D.; Pedersen, L. Particle mesh Ewald: an N-log(N) method for Ewald sums in large systems. *J. Chem. Phys.* **1993**, *98*, 10089–10092.

(31) Ryckaert, J.; Ciccotti, G.; Berendsen, H. J. C. Numerical integration of the cartesian equations of motion of a system with constraints: Molecular dynamics of *n*-alkanes. *J. Comput. Phys.* **1977**, *23*, 327–341.

(32) Lin, T.; Wang, G.; Li, A.; Zhang, Q.; Wu, C.; Zhang, R.; Cai, Q.; Song, W.; Yuen, K. Y. The hemagglutinin structure of an avian H1N1 influenza A virus. *Virology* **2009**, *392*, 73–81.

(33) Kumari, K.; Gulati, S.; Smith, D. F.; Gulati, U.; Cummings, R. D.; Air, G. M. Receptor binding specificity of recent human H3N2 influenza viruses. *Virol. J.* **2007**, *4*, 42–53.

(34) Li, M.; Wang, B. Computational studies of H5N1 hemagglutinin binding with SA-alpha-2, 3-Gal and SA-α-2, 6-Gal. *Biochem. Biophys. Res. Commun.* **2006**, *347*, 662–668.

(35) Xu, D.; Newhouse, E. I.; Amaro, R. E.; Pao, H. C.; Cheng, L. S.; Markwick, P. R.; McCammon, J. A.; Li, W. W.; Arzberger, P. W. Distinct glycan topology for avian and human sialopentasaccharide receptor analogues upon binding different hemagglutinins: A molecular dynamics perspective. *J. Mol. Biol.* **2009**, *387*, 465–491.

(36) Soundararajan, V.; Tharakaraman, K.; Raman, R.; Raguram, S.; Shriver, Z.; Sasisekharan, V.; Sasisekharan, R. Extrapolating from sequence-the 2009 H1N1 "swine" influenza virus. *Nat. Biotechnol.* **2009**, *27*, 510–513.

(37) Coburn, B. J.; Wagner, B. G.; Blower, S. Modeling influenza epidemics and pandemics: insights into the future of swine flu (H1N1). *BMC. Med.* **2009**, *7*, 30–37.

(38) Munster, V. J.; de Wit, E.; van den Brand, J. M.; Herfst, S.; Schrauwen, E. J.; Bestebroer, T. M.; van de Vijver, D.; Boucher, C. A.; Koopmans, M.; Rimmelzwaan, G. F.; Kuiken, T.; Osterhaus, A. D.; Fouchier, R. A. Pathogenesis and transmission of swine-origin 2009 A(H1N1) influenza virus in ferrets. *Science* **2009**, *325*, 481–483.

(39) Maines, T. R.; Jayaraman, A.; Belser, J. A.; Wadford, D. A.; Pappas, C.; Zeng, H.; Gustin, K. M.; Pearce, M. B.; Viswanathan, K.; Shriver, Z. H.; Raman, R.; Cox, N. J.; Sasisekharan, R.; Katz, J. M.; Tumpey, T. M. Transmission and pathogenesis of swine-origin 2009 A(H1N1) influenza viruses in ferrets and mice. *Science* **2009**, *325*, 484–487.

(40) Chen, J.; Fang, F.; Yang, Z.; Liu, X.; Zhang, H.; Zhang, Z.; Zhang, X.; Chen, Z. Characterization of highly pathogenic H5N1 avian influenza viruses isolated from poultry markets in central China. *Virus. Res.* **2009**, *146*, 19–28.

CI100038G